Research Article

Mucize Sarihan*, and Evrim Abamor

Radiation dose measurement on bone scintigraphy and planning clinical management

https://doi.org/10.1515/phys-2022-0211
received September 01, 2022; accepted October 13, 2022

Abstract: Radiation has been used in a variety of different fields since its discovery. It is very important in medial sector for both diagnosis and also for treatment. In this study, the radiation dose rate emitted to the environment after radiopharmaceutical injection was determined using patients undergoing bone scintigraphy imaging. Radiation dose rate measurements were performed at different distances from the patient and at different levels of the patient. Measurements were done at different times to determine the relationship between radiation dose rate and time. The radiation dose rate emitted by the patient was measured after an average of 10.21, 42.36, and 76.28 min of injection. In order to see the relationship between radiation dose rate and distance, measurements were done at 25, 50, 100, and 200 cm distance from the patient. The measured average radiation dose rate at 1 m distance from the patients' chest level and 10.21 min after radiopharmaceutical injection was 16.27 μSv h^{-1}. Then, the average radiation dose rate decayed down to 13.65 μSv h^{-1} after 42.36 min, while the measured average radiation dose rate after 76.28 min was lower as 12.41 μSv h^{-1} at 100 cm from patient's chest level.

Keywords: Tc99m, scintigraphy, radiation dose, hospital management

1 Introduction

Human beings are exposed to natural and artificial radiation throughout their lives. One of the areas where artificial radiation is used is medical applications. Determination of radiation concentration in medical applications is very important for both patients and healthcare workers. Some international organizations have set limits for radiation concentrations that people may be exposed to. It is important for public health that radiation levels in medical applications remain within the recommended limits [1–3].

Radiation effects are of two parts, the definitive deterministic effect and the uncertain stochastic effect. Deterministic effects are the result of high-dose radiation exposure to large body areas. There is a threshold dose value in the deterministic effect formation and the effect increases proportionally with the dose. As a result of this effect, acute radiation syndrome, radiation burns, fibrosis, necrosis, and sclerosis may emerge as late results. Stochastic effects are caused by prolonged exposure to low radiation doses and there is no specific threshold dose value [4].

Bone is in the process of continuous shaping throughout life. Physiological units in bone formation and shaping are osteocytes, osteoblasts, and osteoclasts. Osteoblasts are bone-forming cells. Osteoblasts secrete osteoid which is the main substance of bone. Osteocytes are cells that fill cavities in the bone tissue called lacun. Osteoclasts are separated from hemopoietic progenitor cells. Osteoclasts are specialized macrophages that become powerful phagocytic cells capable of bone resorption in new matrix regions made by osteoblasts [5]. Advanced cancers often metastasize to bone [6]. Bone metastases are most commonly involved in the axial skeleton. The axial skeleton provides a favorable medium for tumor growth due to the large bone marrow, large capillary network, and slow blood flow [7].

Technetium-99m-methylene diphosphonate (Tc-99m MDP) is the most commonly used radiopharmaceutical in bone scintigraphy. Ion exchange occurs between phosphate groups on the surface of the bone matrix and phosphate groups of Tc-99m MDP. Tc-99m is the most widely used radioisotope in nuclear medicine with a half-life of 6 h and emits 140 keV of gamma photons [8].

In this study, static bone scintigraphy was applied on patients with a history of cancer to detect bone metastases. The anamnesis of the patients who apply to the

* **Corresponding author: Mucize Sarihan,** Vocational School of Health Services, Istanbul Okan University, Istanbul, Turkey, e-mail: mucize.sarihan@okan.edu.tr
Evrim Abamor: Nuclear Medicine Department, Dr. Lutfi Kırdar City Hospital, Istanbul, Turkey

clinic for static bone scintigraphy is first taken. After the anamnesis, the radiopharmaceutical (Tc-99m MDP) prepared in the nuclear medicine laboratory is injected into the patient intravenously. In bone scintigraphy imaging, adult patients are injected intravenously with 20–30 mCi (740–1,110 MBq) radiopharmaceutical (Tc-99m MDP).

While the prepared radiopharmaceutical is applied to the patient, the employees wear a lead apron and inject with the injectors in the lead shield. The patient is taken to the radioactive waiting room within the framework of time, distance, and shielding measures, which are three important factors in radiation protection. Patients are kept in the radioactive waiting room for 1.5–2 h for better retention of Tc-99m radioactivity. The accompanying relatives of the patient are kept outside the room. Meanwhile, the patient is given 2 L of water. The patients drinking water is important for the involvement of the radiopharmaceutical. The patient waiting for a minimum of 1.5 h is told to empty his bladder and then the patient is taken to the imaging room. After administering the radiopharmaceutical, it is important that the patient be kept as far as possible from healthcare professionals and other patients during waiting, imaging, and after imaging. In addition, using lead shielding will cause employees to be affected by less radiation.

Radiation exposure hazards are regulated by the International commission on radiological protection (ICRP). ICRP recommended a radiation dose rate of 20 $\mu Sv\ h^{-1}$ at a distance of 1 m from the patient to allow patients to be discharged after radionuclide treatment [9]. Therefore, it is really important to investigate the concentration of radiation emitted from the patient and the expected dose rate after radiopharmaceutical injection in nuclear medicine.

Some studies have been carried out on the radiation doses emitted to the environment after different radiopharmaceuticals were injected to the patients. In these studies, usually the doses they emit into the environment after FDG injection were examined.

Sometimes, patients injected with radiopharmaceuticals do not know the exact time and distance of approaching other people. The main motivation of this study is to determine the time and distance that can be approached to the patient emitting radiation. This time and distance are very important especially for the relatives of the patients.

The main purpose of this study was to determine the radiation dose rate emitted by patients undergoing bone scintigraphy. The radiation dose rate emitted by the patient varies with time and distance from the patient. In order to determine the change in radiation dose rate over time and distance, measurements were done after different periods of radiopharmaceutical injection and at different distances from the patient.

2 Materials and methods

This study was carried out in Istanbul Dr Lutfu Kırdar City Hospital, Nuclear Medicine Department. The study was conducted on 25 people (13 females and 12 males) whose ages ranged from 38 to 92 years (mean 60.33 years). The weight of the participants ranged from 49 to 130 kg, with an average of 75.78 kg .

Patients were first injected with radiopharmaceuticals by weight. The radioactivity given to patients ranged from 17.23 mCi (637.51 MBq) to 20.58 mCi (761.46 MBq), with an average of 19.06 mCi (705.22 MBq). Immediately after radiopharmaceutical injection, patients began to emit radiation around them.

Patients undergoing bone scintigraphy imaging were used to calculate the external radiation dose rate after radiopharmaceutical injection in this investigation. Radiation dose rates were measured from a variety of angles and at a variety of distances from the patient. For this study, we took readings at various intervals to establish a time–dosimetry relationship for the radiation dosage rate. After an average of 10.21, 42.36, and 76.28 min post-injection, the patient's radiation dosage rate was measured. Experiments were performed at 25, 50, 100, and 200 cm from the patient to determine the dose rate as a function of distance.

The radiation dose rate emitted by the patient was measured after an average of 10.21, 42.36, and 76.28 min after injection. In order to determine the relationship between radiation dose rate and distance, measurements were done at 25 cm distance, 50 cm distance, 100 cm distance, and 200 cm distance from the patient (Figure 1). As shown in Figure 1, the measurement places are labelled as HL-25 which is 25 cm distance from patient's head level, HL-50 is 50 cm distance from patient's head level, HL-100 is 100 cm distance from patient's head level, HL-200 is 200 cm distance from patient's head level, CL-25 is 25 cm distance from patient's chest level, CL-50 is 50 cm distance from patient's chest level, CL-100 is 100 cm distance from patient's chest level, CL-200 is 200 cm distance from patient's chest level, FL-25 is 25 cm distance from patient's foot level, FL-50 is 50 cm distance from patient's foot level, FL-100 is 100 cm distance from patient's foot level, and FL-200 is 200 cm distance from patient's foot level.

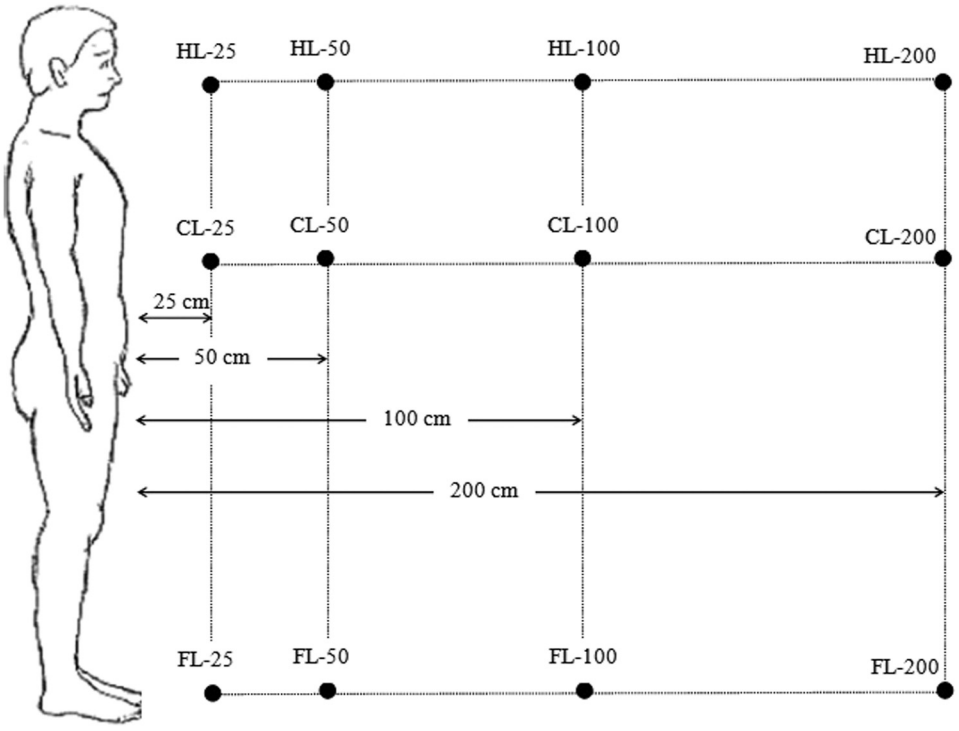

Figure 1: Locations of measurements performed on human body.

Radiation rate measurements at the head level were done at 25, 50, 100, and 200 cm distances from the patient's head level. Radiation rate measurements at the chest level were done at 25, 50, 100, and 200 cm distances from the patient's chest level. Radiation rate measurements at the foot level were done at 25, 50, 100, and 200 cm distances from the patient's foot level. Thus, the radiation dose rate was determined from 12 different points around the patient. Radiation dose rate measurements were performed using the GM (Inspector Nuclear Radiation Monitor Deluxe Dose Rate CPT.5250-0047) detector which was calibrated by Turkey Atomic Energy Agency.

3 Results and discussion

The average radiation dose rate at 25, 50, 100, and 200 cm from the patient's head level is shown in Table 1. The average radiation dose rate measured at 1 m distance from the patients' head level and 10.21 min after radiopharmaceutical injection was 14.56 μSv h^{-1} (range 8.26–19.17). Then, the average radiation dose rate decayed down to 12.89 μSv h^{-1} (range 8.13–17.43) after 42.36 min, while the measured average radiation dose rate after 76.28 min was lower at 10.72 μSv h^{-1} (range 5.37–15.67) at 100 cm from patient's head level.

Table 1: Radiation dose rates at patient's head level at different distances and at different times after injection

Distance from patient (cm)	Time after the injection (min)	Dose rate range (μSv h^{-1})	Mean dose rate (μSv h^{-1})	Normalized mean dose rate (μSv h^{-1} MBq^{-1})
25	10.21	45.16–140.23	68.11	0.0966
	42.36	24.67–90.35	53.27	0.0755
	76.28	15.63–78.26	47.01	0.0667
50	10.21	19.35–37.81	28.16	0.0399
	42.36	17.53–31.48	23.61	0.0335
	76.28	12.67–24.59	18.83	0.0267
100	10.21	8.26–19.17	14.56	0.0206
	42.36	8.13–17.43	12.89	0.0183
	76.28	5.37–15.67	10.72	0.0152
200	10.21	5.83–10.56	7.38	0.0105
	42.36	4.23–10.38	6.01	0.0085
	76.28	3.41–9.26	5.68	0.0081

The average radiation dose rate at 25, 50, 100, and 200 cm from the patient's chest level is shown in Table 2. The average radiation dose rate measured at 1 m distance from the patients' chest level and 10.21 min after radiopharmaceutical injection was 16.27 μSv h^{-1} (range 7.83–24.71). Then, the average radiation dose rate decayed down to 13.65 μSv h^{-1}(range 7.12–21.43) after 42.36 min, while the

Table 2: Radiation dose rates at patient's chest level at different distances and at different times after injection

Distance from patient (cm)	Time after the injection (min)	Dose rate range (μSv h^{-1})	Mean dose rate (μSv h^{-1})	Normalized mean dose rate (μSv h^{-1} MBq^{-1})
25	10.21	61.83–172.29	124.33	0.1763
	42.36	44.97–155.43	99.13	0.1406
	76.28	38.43–143.52	78.13	0.1108
50	10.21	23.97–81.26	44.16	0.0626
	42.36	22.63–54.78	38.38	0.0544
	76.28	21.34–48.53	33.44	0.0474
100	10.21	7.83–24.71	16.27	0.0231
	42.36	7.12–21.43	13.65	0.0194
	76.28	6.43–19.36	12.41	0.0176
200	10.21	4.38–9.56	8.41	0.0119
	42.36	4.13–9.12	6.43	0.0091
	76.28	4.01–9.07	6.36	0.0090

measured average radiation dose rate after 76.28 min was lower at 12.41 μSv h^{-1} (range 6.43–19.36) at 100 cm from patient's chest level.

The average radiation dose rate measured at 1 m distance from the patients' foot level and 10.21 min after radiopharmaceutical injection was 13.38 μSv h^{-1} (range 7.52–19.68). Then, the average radiation dose rate decayed down to 12.34 μSv h^{-1} (range 7.41–17.59) after 42.36 min, while the measured average radiation dose rate after 76.28 min was lower at 11.16 μSv h^{-1} (range 5.98–15.43) at 100 cm from patient's foot level. The obtained results are tabulated in Table 3.

Table 3: Radiation dose rates at patient's foot level at different distances and at different times after injection

Distance from patient (cm)	Time after the injection (min)	Dose rate range (μSv h^{-1})	Mean dose rate (μSv h^{-1})	Normalized mean dose rate (μSv h^{-1} MBq^{-1})
25	10.21	26.89–92.51	46.94	0.0666
	42.36	20.13–66.34	40.38	0.0573
	76.28	18.96–56.31	32.27	0.0458
50	10.21	16.53–45.86	23.55	0.0334
	42.36	14.56–30.08	21.05	0.0298
	76.28	7.89–26.52	18.66	0.0265
100	10.21	7.52–19.68	13.38	0.0190
	42.36	7.41–17.59	12.34	0.0175
	76.28	5.98–15.43	11.16	0.0158
200	10.21	3.97–9.53	6.12	0.0087
	42.36	3.72–9.32	5.78	0.0082
	76.28	3.04–7.53	5.27	0.0075

10.21 min after radiopharmaceutical injection to the patient, it was observed that the radiation dose rate decreased as the distance from the patient increased. Measurements at head, chest, and foot levels showed strong correlations between distance from the patient and radiation dose rate. Correlation coefficients were 0.995 for head level, 0.990 for chest level, and 0.996 for foot level (Figure 2).

42.36 min after injection to the patient, radiation dose rate decreased as the distance from the patient increased. Measurements at head, chest, and foot levels showed strong correlations between distance from the patient and radiation dose rate. Correlation coefficients were 0.997 for head level, 0.996 for chest level, and 0.995 for foot level (Figure 3).

76.28 min after injection to the patient, radiation dose rate decreased as the distance from the patient increased. Measurements at head, chest, and foot levels showed strong correlations between distance from the patient and radiation dose rate. Correlation coefficients were

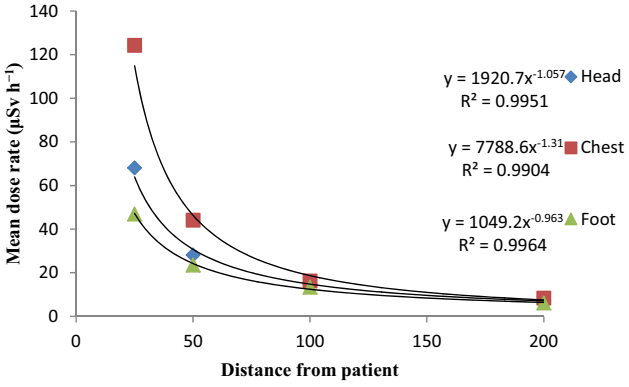

Figure 2: 10.21 min after injection, the patient's head, chest, and foot radiation dose rates.

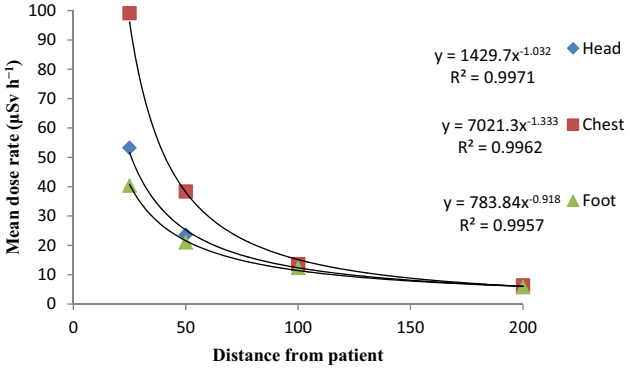

Figure 3: 42.36 min after injection, the patient's head, chest, and foot radiation dose rates.

0.988 for head level, 0.994 for chest level, and 0.992 for foot level (Figure 4).

Radiation dose rate measurements at the patient's head level were found to decrease with the increase in time. In the measurements at the head level, the correlation coefficients between radiation dose rate and time at 25, 50, 100, and 200 cm distances from the patient were 0.960, 0.996, 0.989, and 0.893, respectively (Figure 5).

Radiation dose rate measurements at the patient's chest level were found to decrease with the increase in time. In the measurements at the chest level, the correlation coefficients between the radiation dose rate and time at 25, 50, 100, and 200 cm distances from the patient were 1, 0.999, 0.966, and 0.766, respectively (Figure 6).

Radiation dose rate measurements at the patient's foot level were found to decrease with the increase in time. In the measurements at the foot level, the correlation coefficients between radiation dose rate and time at 25, 50, 100, and 200 cm distances from the patient were 0.990, 1, 0.997, and 0.985, respectively (Figure 7). The radiation dose rate distribution 10.21, 42.36, and 76.28 min after radiopharmaceutical injection to the patient is shown in Figures 8–10.

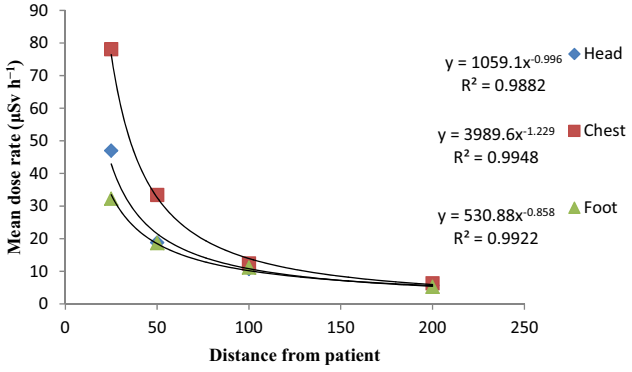

Figure 4: 76.28 min after injection, the patient's head, chest, and foot radiation dose rates.

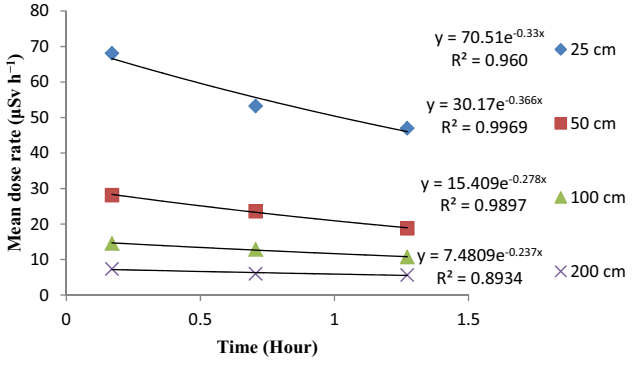

Figure 5: Radiation dose rate at different distances from the patient's head level.

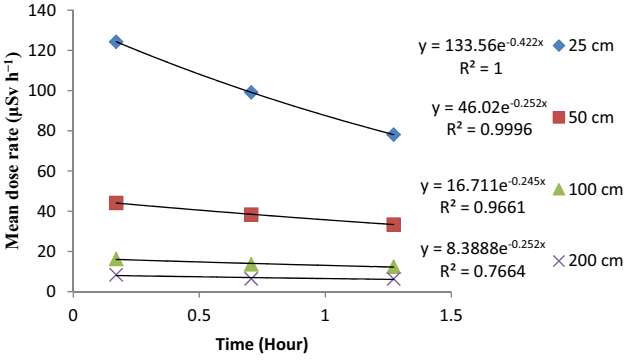

Figure 6: Radiation dose rate at different distances from the patient's chest level.

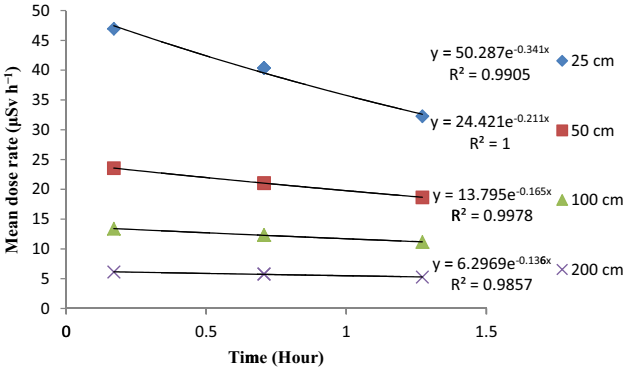

Figure 7: Radiation dose rate at different distances from the patient's foot level.

Demir *et al.* found that in 2010, 87 min after the patient was injected with 550 MBq FDG, the radiation dose rate at a distance of 1 m from the patient was 74 μSv h^{-1} [10]. Cronin *et al.* found that in 1999, 120 min after the patient was injected with 323 MBq FDG, the radiation dose rate at a distance of 1 m from the patient was 14.7 μSv h^{-1} [11]. Zhang-Yin *et al.* found that in 2017, 95 min after the patient was injected with 176 MBq FDG, the radiation dose rate at a distance of 1 m from the patient was 9.34 μSv h^{-1} [12]. Gunay and Abamor found that in 2018, 77 min after the patient was injected with 300 MBq FDG, the radiation dose rate at a distance of 1 m from the patient was 15 μSv h^{-1} [13].

Günay *et al.* investigated the radiation dose rates at different distances from the patient after injecting Tc-99m in two different studies in 2019 [14,15]. One of these studies was performed on cardiac patients. In this study conducted by Günay *et al.*, 276 MBq radiopharmaceuticals were injected to the patients. Radiation dose rate was measured at a distance of 1 m from patients. Radiation

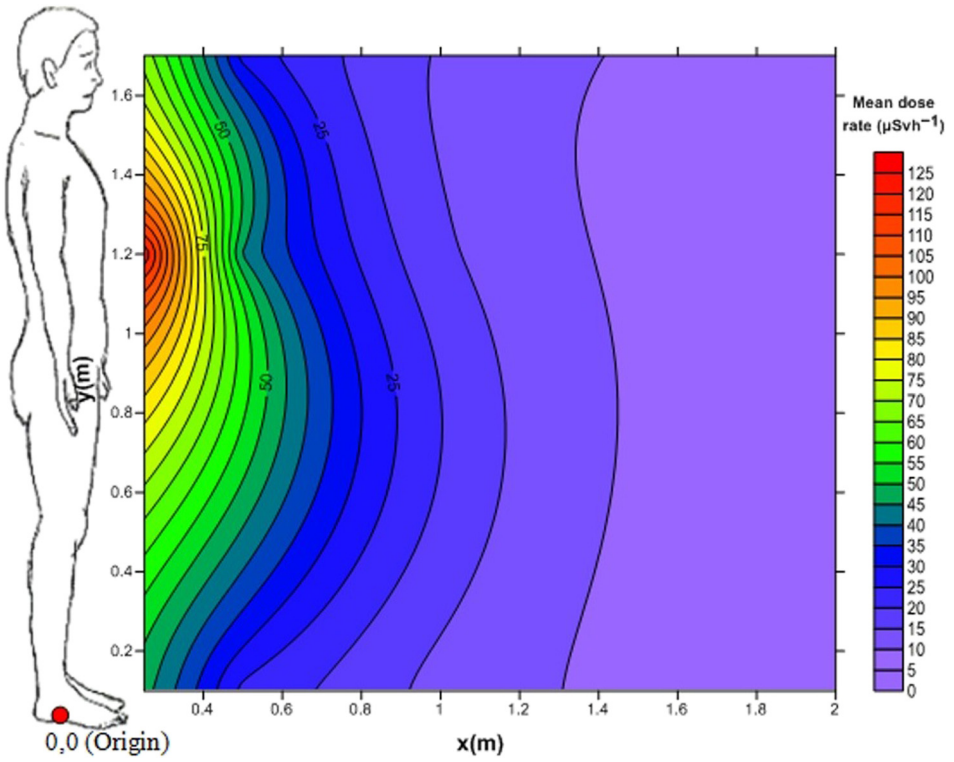

Figure 8: Radiation dose rate distribution at 10.21 min after injection.

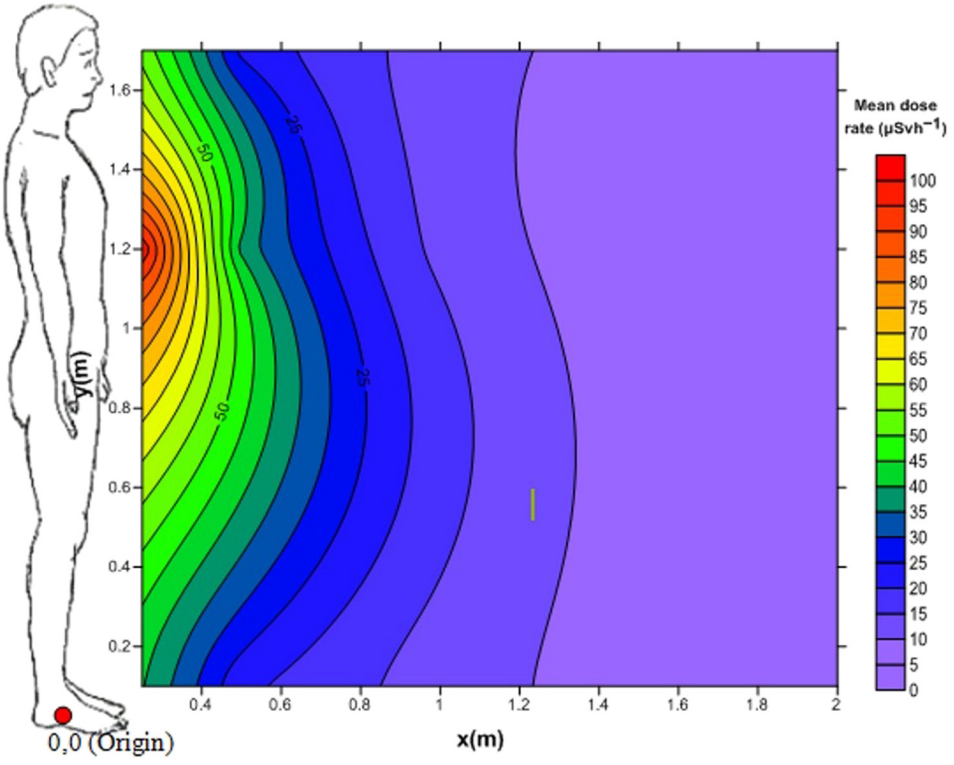

Figure 9: Radiation dose rate distribution at 42.36 min after injection.

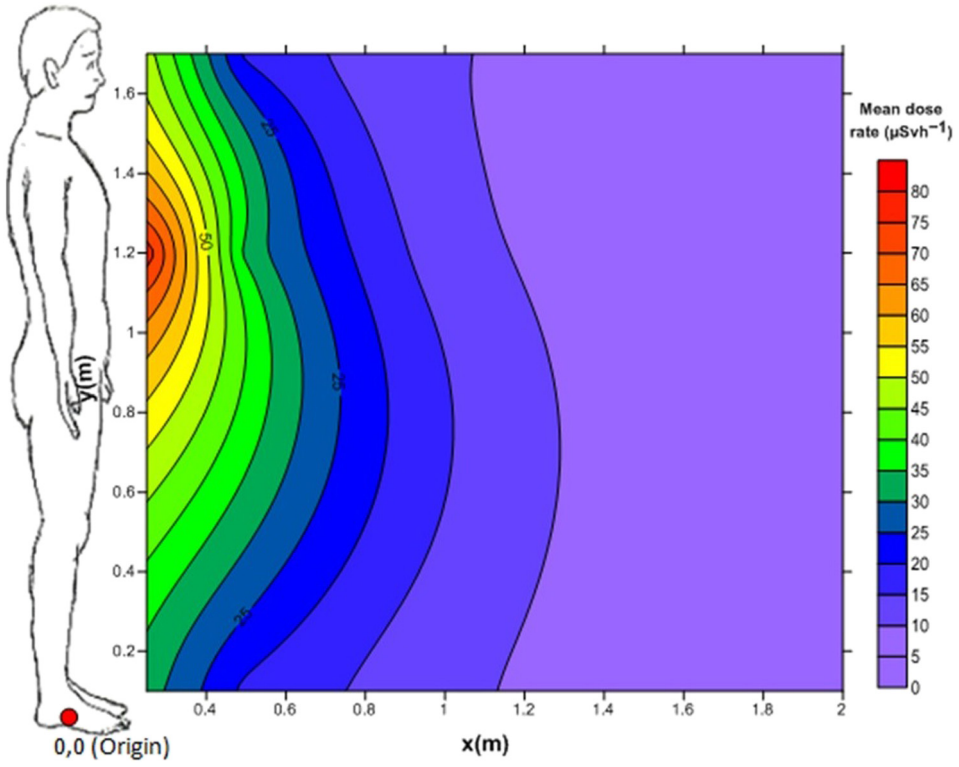

Figure 10: Radiation dose rate distribution at 76.28 min after injection.

dose rates at 7.6, 36.5, and 66.4 min after injection were 9.07, 7.93, and 7.83 μSv h^{-1}, respectively. In the other study, environmental radiation doses were determined in patients undergoing Tc-99m DMSA cortical renal scintigraphy. In this study conducted by Günay *et al.*, 168 MBq radiopharmaceuticals were injected to the patients. Radiation dose rate was measured at a distance of 1 m from patients. The mean radiation dose at 5.07, 35.60, and 68.57 min after injection were found to be 5.06, 4.76, and 4.18 μSv h^{-1} at a distance of 1 m from the patients, respectively. Besides those of previous works, a number of radiation dose measurements and dosimetric studies have been performed for different purposes by different groups [16–38].

Since radiation containing different amounts of activity was injected into patients in different previous studies, depending on the type of disease, the dose rate emitted from the patient was found to be different in each study. The radiation dose rate results in this study were found to be higher than some previous similar studies and lower than others.

4 Conclusion

In this study, the radiation dose rate emitted to the environment after radiopharmaceutical injection was determined by patients undergoing bone scintigraphy imaging. Radiation dose rate measurements were made at different distances from the patient and at different levels of the patient. Measurements were made at different times to determine the relationship between radiation dose rate and time. A safe time and distance were determined for radiation workers and the public to approach patients who underwent bone scintigraphy.

Radiation worker should be exposed to less than 10 μSv h^{-1} dose [39]. Radiation workers should stay 1 m away from the patient for 130 min after radiopharmaceutical injection during bone scintigraphy imaging.

Radiation dose rate for the public should be less than 1 μSv h^{-1}. According to the equation between the radiation dose rate of 1 m from the patient's chest level and time, 130 min after radiopharmaceutical injection, the radiation dose rate of 1 m from the patient is less than 1 μSv h^{-1}. Therefore, following bone scintigraphy applications, it is appropriate for the patient to restrain social activities such as being 1 m away from other people and using public transport, for at least 130 min after injection. In nuclear medicine, radiation of different activities is injected for different diseases. In future studies, it is recommended to measure the radiation dose rates emitted by patients injected with radiation of different activities.

Funding information: The authors state no funding involved.

Author contributions: All authors have accepted responsibility for the entire content of this manuscript and approved its submission.

Conflict of interest: The authors state no conflict of interest.

Ethical approval: The research related to human use has been complied with all the relevant national regulations, institutional policies and in accordance with the tenets of the Helsinki Declaration, and has been approved by the authors' institutional review board or equivalent committee.

References

[1] Günay O. Assessment of lifetime cancer risk from natural radioactivity levels in Kadikoy and Uskudar districts of Istanbul. Arab J Geosci. 2018;11:1–6. doi: 10.1007/s12517-018-4151-9.
[2] Palaci H, Günay O, Yarar O. Evaluation of radiation safety and protection training in Turkey. Eur J Sci Technol. 2018;249–54. doi: 10.31590/ejosat.479367.
[3] Kuru L, Günay O, Palacı H, Yarar O. Determination of the effective radiation dose of the patient in computed tomography. Balıkesir Ünive Fen Bilim Enstit Derg. 2019;21:436–43. doi: 10.25092/baunfbed.548627.
[4] Noureldin YA, Andonian S. Radiation safety during diagnosis and treatment. Smith's Textb Endourol. 2019;14–37. doi: 10.1002/9781119245193.ch2
[5] Parfitt AM. Bone remodeling, normal and abnormal: a biological basis for the understanding of cancer-related bone disease and its treatment. Can J Oncol. 1995;5(Suppl 1):1–10.
[6] Brown JE, Neville-Webbe H, Coleman RE. The role of bisphosphonates in breast and prostate cancers. Endocr Relat Cancer. 2004;11:207–24. doi: 10.1677/erc.0.0110207.
[7] Rosenthal DI. Radiologic diagnosis of bone metastases. Cancer. 1997;80:1595–607. doi: 10.1002/(SICI)1097-0142(19971015)80:8+<1595:AID-CNCR10>3.0.CO;2-V.
[8] Kekilli E, Yağmur C, Ertem K, Bilen TB. Nuclear medicine applications in bone grafts. Turkiye Klinikleri J Med Sci. 2005;25(2):261–79.
[9] Abuqbeitah M, Demir M, Çavdar İ, Tanyildizi H, Yeyin N, Uslu-Beşli L, et al. Red bone marrow dose estimation using several internal dosimetry models for prospective dosimetry-oriented radioiodine therapy. Radiat Env Biophys. 2018;57:395–404. doi: 10.1007/s00411-018-0757-2.
[10] Demir M, Demir B, Sayman H, Sager S, Sabbir Ahmed A, Uslu I. Radiation protection for accompanying person and radiation workers in PET/CT. Radiat Prot Dosim. 2011;147:528–32. doi: 10.1093/rpd/ncq497.
[11] Cronin B, Marsden PK, O'Doherty MJ. Are restrictions to behaviour of patients required following fluorine-18 fluorodeoxyglucose positron emission tomographic studies? Eur J Nucl Med. 1999;26:121–8. doi: 10.1007/s002590050367.
[12] Zhang-Yin J, Dirand AS, Sasanelli M, Corrégé G, Peudon A, Kiffel T, et al. Equivalent dose rate 1 meter from neuroendocrine tumor patients exiting the nuclear medicine department after undergoing imaging. J Nucl Med. 2017;58:1230–5. doi: 10.2967/jnumed.116.187138.
[13] Günay O, Abamor E. Environmental radiation dose rate arising from patients of PET/CT. Int J Env Sci Technol. 2019;16:5177–84. doi: 10.1007/s13762-018-2040-0.
[14] Günay O, Sarihan M, Abamor E, Yarar O. Environmental radiation doses from patients undergoing Tc-99m DMSA cortical renal scintigraphy. Int J Comput Exp Sci Eng. 2019;5:86–93. doi: 10.22399/ijcesen.589267.
[15] Günay O, Sarıhan M, Yarar O, Abuqbeitah M, Demir M, Sönmezoğlu K, et al. Determination of radiation dose from patients undergoing Tc-99m Sestamibi nuclear cardiac imaging. Int J Env Sci Technol. 2019;16:5251–8. doi: 10.1007/s13762-019-02262-1.
[16] Albidhani H, Gunoglu K, Akkurt İ. Natural Radiation Measurement in Some Soil Samples from Basra oil field, IRAQ State. Int J Comput Exp Sci Eng. 2019;5(1):48–51. doi: 10.22399/ijcesen.498695.
[17] Çelen YY. Gamma ray shielding parameters of some phantom fabrication materials for medical dosimetry. Emerg Mater Res. 2021;10(3):307–13. doi: 10.1680/jemmr.21.00043.
[18] Tekin HO, Cavli B, Altunsoy EE, Manici T, Ozturk C, Karakas HM. An investigation on radiation protection and shielding properties of 16 slice computed tomography (CT) facilities. Int J Comput Exp Sci Eng. 2018;4(2):37–40. doi: 10.22399/ijcesen.408231.
[19] Ucar M, Kayıran Hüseyin F, Korkmaz AV. Gamma ray shielding parameters of carbon-aramid epoxy composite. Emerg Mater Res. 2022;11(3):338–44. doi: 10.1680/jemmr.22.00072.
[20] Demir N, Kivrak A, Üstün M, Cesur A, Boztosun I. Experimental study for the energy levels of Europium by the clinic LINAC. Int J Comput Exp Sci Eng. 2017;3(1):47–9.
[21] Altunsoy EE, Tekin HO, Mesbahi A, Akkurt I. MCNPX simulation for radiation dose absorption of anatomical regions and some organs. Acta Phys Polonica A. 2020;137(4):561. doi: 10.12693/APhysPolA.137.561.
[22] El-Agawany FI, Mahmoud KA, Akyildirim H, Yousef ES, Tekin HO, Rammah YS. Physical, neutron, and gamma-rays shielding parameters for Na_2O–SiO_2–PbO glasses. Emerg Mater Res. 2021;10(2):227–37. doi: 10.1680/jemmr.20.00297.
[23] Akkurt İ, Uyanik NA, Günoğlu K. Radiation dose estimation: An *in vitro* measurement for Isparta-Turkey. Int J Comput Exp Sci Eng. 2015;1(1):1–4. doi: 10.22399/ijcesen.194376.
[24] Günay O, Eke C. Determination of terrestrial radiation level and radiological parameters of soil samples from Sariyer-Istanbul in Turkey. Arab J Geosci. 2019;12:631. doi: 10.1007/s12517-019-4830-1.
[25] Akkurt I. Effective atomic numbers for Fe–Mn alloy using transmission experiment. Chin Phys Lett. 2007;24:2812. doi: 10.1088/0256-307X/24/10/027.
[26] Tekin HO, ALMisned G, Susoy G, Zakaly HM, Issa SA, Kilic G, et al. A detailed investigation on highly dense CuZr bulk metallic

glasses for shielding purposes. Open Chem. 2020;20(1):69–80. doi: 10.1515/chem-2022-0127.
[27] Akkurt I. Effective atomic and electron numbers of some steels at different energies. Ann Nucl En. 2009;36(11–12):1702–5. doi: 10.1016/j.anucene.2009.09.005.
[28] Günay O, Gündoğdu Ö, Demir M, Abuqbeitah M, Yaşar D, Aközcan S, et al. Determination of the radiation dose level in different slice computerized tomography. Int J Comput Exp Sci Eng. 2019;5(3):119–23. doi: 10.22399/ijcesen.595645.
[29] Demir N, Tarim UA, Popovici MA, Demirci ZN, Gurler O, Akkurt I. Investigation of mass attenuation coefficients of water, concrete and bakelite at different energies using the FLUKA Monte Carlo code. J Radioanal Nucl Chem. 2013;298:1303–7. doi: 10.1007/s10967-013-2494-y.
[30] Akkurt I, Akyıldırım H, Karipçin F, Mavi B. Chemical corrosion on gamma-ray attenuation properties of barite concrete. J Saudi Chem Soc. 2012;6(2):199–202. doi: 10.1016/j.jscs.2011.01.003.
[31] Waheed F, İmamoğlu M, Karpuz N, Ovalıoğlu H. Simulation of Neutrons Shielding Properties for Some Medical Materials. Int J Comput Exp Sci Eng. 2022;8(1):5–8. doi: 10.22399/ijcesen.1032359.
[32] Tekin HO, ALMisned G, Zakaly HM, Zamil A, Khoucheich D, Bilal G, et al. Gamma, neutron, and heavy charged ion shielding properties of Er^{3+}-doped and Sm^{3+}-doped zinc borate glasses. Open Chem. 2022;20(1):130–45. doi: 10.1515/chem-2022-0128.
[33] Etyemez A. Structural, physical, and mechanical properties of the TiO_2 added hydroxyapatite composites. Open Chem. 2022;20(1):272–6. doi: 10.1515/chem-2022-0140.
[34] Awad HA, El-Leil IA, Nastavkin AV, Tolba A, Kamel M, El-Wardany RM, et al. Statistical analysis on the radiological assessment and geochemical studies of granitic rocks in the north of Um Taghir area, Eastern Desert, Egypt. Open Chem. 2022;20(1):254–66. doi: 10.1515/chem-2022-0131.
[35] Boodaghi Malidarre R, Akkurt İ, Gunoglu K, Akyıldırım H. Fast neutrons shielding properties for HAP-Fe_2O_3 composite materials. Int J Comput Exp Sci Eng. 2021;7(3):143–5. doi: 10.22399/ijcesen.1012039.
[36] Sarihan M. Simulation of gamma-ray shielding properties for materials of medical interest. Open Chem. 2022;20(1):81–7. doi: 10.1515/chem-2021-0118.
[37] Oruncak B. Gamma-ray Shielding Properties of Nd_2O_3 added Iron-Boron-Phosphate based composites. Open Chem. 2022;20(1):237–43. doi: 10.1515/chem-2022-0143.
[38] Kamar MS, Salem IA, El-Aassy IE, El-Sayed AA, Awad HA, Tekin HO, et al. Petrology and geochemistry of multiphase post-granitic dikes: A case study from Gabal Serbal area, Southwestern Sinai, Egypt. Open Chem. 2022;20(1):169–81. doi: 10.1515/chem-2022-0136.
[39] Demir M. Radiobiological effects, protection of the patient, protection of caregivers, protection of those around the patient and the environment. Nucl Med Semin. 2015;1:171–9. doi: 10.4274/nts.0026.